Hemapala, K. T. M. U.; Swathika, O.V. Gnana; Dharmadasa, K. P. R. D. S. K.

Article

Techno-economic feasibility of lighting protection of overhead transmission line with multi-chamber insulator arrestors

Development Engineering

Provided in Cooperation with:
Elsevier

Suggested Citation: Hemapala, K. T. M. U.; Swathika, O.V. Gnana; Dharmadasa, K. P. R. D. S. K. (2018) : Techno-economic feasibility of lighting protection of overhead transmission line with multi-chamber insulator arrestors, Development Engineering, ISSN 2352-7285, Elsevier, Amsterdam, Vol. 3, pp. 100-116, https://doi.org/10.1016/j.deveng.2018.05.003

Development Engineering 3 (2018) 100–116

Contents lists available at ScienceDirect

Development Engineering

journal homepage: www.elsevier.com/locate/deveng

Techno-economic feasibility of lighting protection of overhead transmission line with multi-chamber insulator arrestors

K.T.M.U. Hemapala [a], O.V. Gnana Swathika [b,*], K.P.R.D.S.K. Dharmadasa [a]

[a] University of Moratuwa, Moratuwa, Sri Lanka
[b] School of Electrical Engineering, VIT University, Chennai, India

ARTICLE INFO

Index Terms:
Lightning protection
Overhead transmission line
Multi-chamber insulator arrestor

ABSTRACT

The performance of transmission lines has a significant impact on reliability aspects of the power supply system of a country. The lightning back flashover effects are recognized as one of the major causes of transmission line outages. This paper focuses on studying the effect of Multi Chamber Insulator Arresters (MCIA) on lightning back flashover by transient modeling and subsequent simulation of a selected transmission line. Power System CAD (PSCAD) software program is utilized as the software tool for modeling and simulation of the 132 kV, Matugama-Kukule transmission line for this study. Simulation of the created transmission line model is carried out with and without MCIA to evaluate the improvements in lightning back flashover performance after installation of MCIAs in this transmission line. This analysis will contribute to improve the reliability of the Sri Lankan electrical power system.

1. Introduction

A lightning stroke terminating in the shield wires produces waves of currents and voltages travelling on the shield wires known as travelling waves, and reflections occurs at every points where the impedance is discontinuous (Statistical Digest, 2014, 2014; Datsios et al., 2014). The occurrence of component failures due to lightning are predominant in areas where there is significantly high keraunic level. Grounding devices with low impedance and huge quantum of current carrying capability are suggested in (Ekonomou et al., 2007; Minnaar et al., 2012; Visacro et al., 2012) as a solution.

Direct lightning triggers insulation failure, but indirect lightning are more frequent in the presence of tall structures. Most literature focuses on indirect lightning performance which is challenging in terms of computation and it requires solving the field-to-line coupling iteratively before assuming the stochastic variables. It is hence necessary to identify the optimal spacing to be maintained between arrestors (Banjanin et al., 2015; Protection against lightn, 2006a; Visacro and Alipio, 2012; Protection against lightn, 2006b; Napolitano et al., 2016).

The surge voltages that maybe developed across the line insulators due to lightning could exceed the Critical Flashover Voltage (CFO) (Mikropoulos et al., 2014; Napolitano et al., 2014; De Conti et al., 2010). Towers which have high tower footing resistance in lightning prone areas have higher probability of back-flashover occurrence and the cases are worst in hilly terrains (Maslowski et al., 2016; Napolitano et al., 2015; Wu et al., 2016; Jinpeng et al., 2015; Visacro et al., 2011; Brignone et al., 2017a). Back-flashovers occur frequently in overhead lines (OHL) with ground wires. (Chen and Zhu, 2014; Brignone et al., 2012, 2014, 2017b; Andreotti et al., 2015; Banjanin, 2018).

A simulation model is created using the electromagnetic transient analysis subcomponent of PSCAD/EMTDC, which depicts the transmission system as a collection of tower, insulator, transmission line and grounding devices, in order to determine the optimal way of protecting the transmission system from direct lightning. Most of the transmission lines in Sri Lanka traverse through hilly terrains prone to heavy lightning as a result of which many lines are prone to back flashover problems which reduce transmission system reliability. Kukule-Matugama, 132 kV transmission line is one such line that experiences back-flashovers very frequently. As a result, the Kukule Power Station (35 MW X 2) is separated from the transmission network most of the time causing low system reliability. This paper analyzes the back-flashover of Kukule-Mathugama, 132 kV transmission line by performing transient modeling and

* Corresponding author.
E-mail addresses: udayanga@elect.mrt.ac.lk (K.T.M.U. Hemapala), gnanaswathika.ov@vit.ac.in (O.V. Gnana Swathika), dhammika.dharmadasa@gmail.com (K.P.R.D.S.K. Dharmadasa).

https://doi.org/10.1016/j.deveng.2018.05.003
Received 2 March 2017; Received in revised form 4 May 2018; Accepted 4 May 2018
Available online 8 May 2018

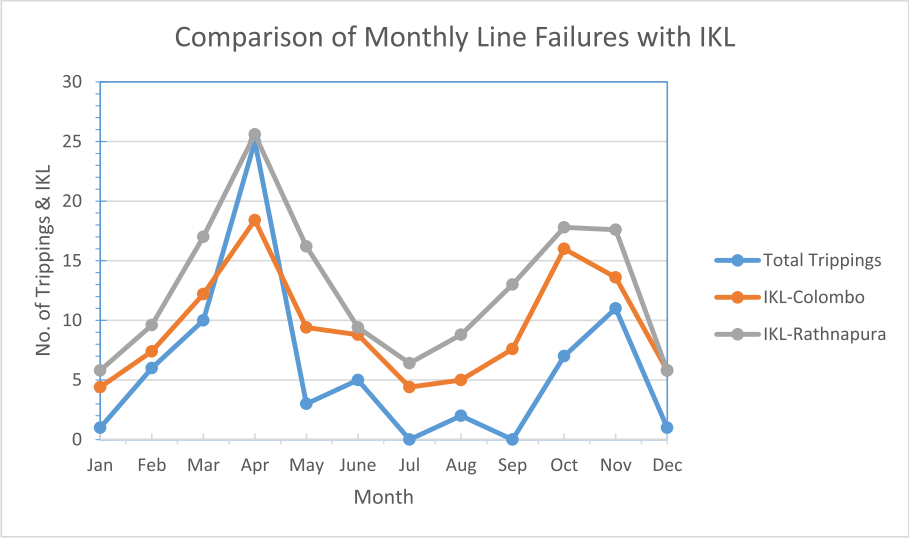

Fig. 1. Comparison of monthly line failures with IKL

simulation. The network is simulated with and without the Multi Chamber Insulator Arresters (MCIA) in the model. The improvement in lightning back-flashover performance is also evaluated after installation of the MCIAs in the selected transmission line.

Section 2 discusses the problem formulation of this paper which highlights the necessity to avoid double circuit failures in transmission line. Section 3 elaborates the complete line model along with MCIA model and back flashover control model using EMTP/PSCAD. It also depicts the method of simulation incorporated in the models. Section 4 showcases the behavior of transmission line with and without MCIA model. It also specifies the optimum location at which the MCIA models may be placed to eradicate the back-flashover event. This section also indicates electrical and mechanical properties of the insulator used in the transmission network.

2. Problem formulation

The selected 132 kV, Matugama-Kukule transmission line is a double circuit line which delivers the power generated by the Kukule Power Station (35 MW * 2) to the national grid. Since a single circuit of Lynx conductor carries approximately 80 MW of power at the rated voltage, the full power output of the power plant may be transmitted even with the tripping of single circuit. Therefore, only the tripping of both circuits is considered for the analysis. Kukule Power Station is used only during the peak load and a sudden outage of this power station creates a drop in the system frequency. In such situations, the loss of generation is recovered from the spinning reserve. The loss of Kukule generation tends to create low voltages in the southern part of the transmission network and in some occasions under frequency load shedding schemes may also have to be activated. Therefore, it is of utmost importance to avoid any double circuit failures by improving the lightning performance of the selected Matugama-Kukule transmission line to avoid partial failures of the power system and the associated heavy financial losses.

According to the past performance records of this transmission line, it is evident that the failure of this transmission line subjects a great influence on the partial failures of the system. It is observed that most of the line outages are due to the effect of frequent lightning strikes that are recorded during April to June and October to November. Fig. 1 illustrates the relationship of Isokaraunic Level (IKL) with the number of transmission line failures in each month.

Reduction in the tower earthing resistance is a key solution to avoid back-flashovers. However, it is not practical and economical when the towers are located at hilly areas where the soil condition is poor. Another solution for preventing back-flashover is by adopting unbalanced or improved line insulation. But this solution proves uneconomical due to the requirement of additional insulator discs which may need modifications in the towers. It is found that the most economical and effective way of preventing back-flashovers is to install Transmission Line Arresters (TLA) at selected tower locations. However, installing TLAs also need special preparations of cross arms or special means of installing on

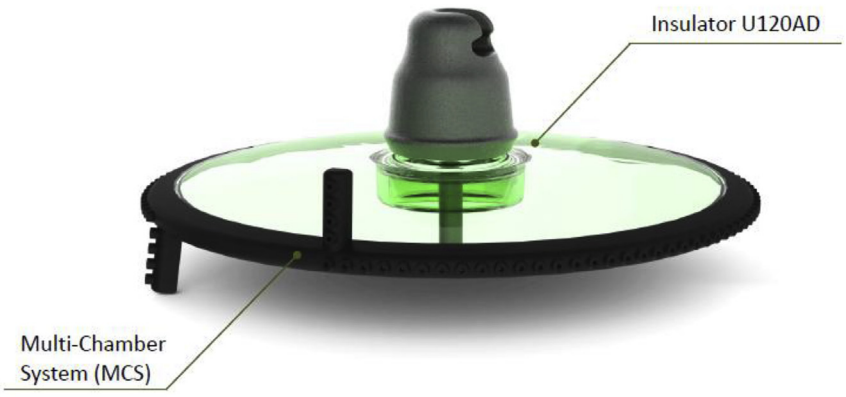

Fig. 2. U120D Glass MCIA.

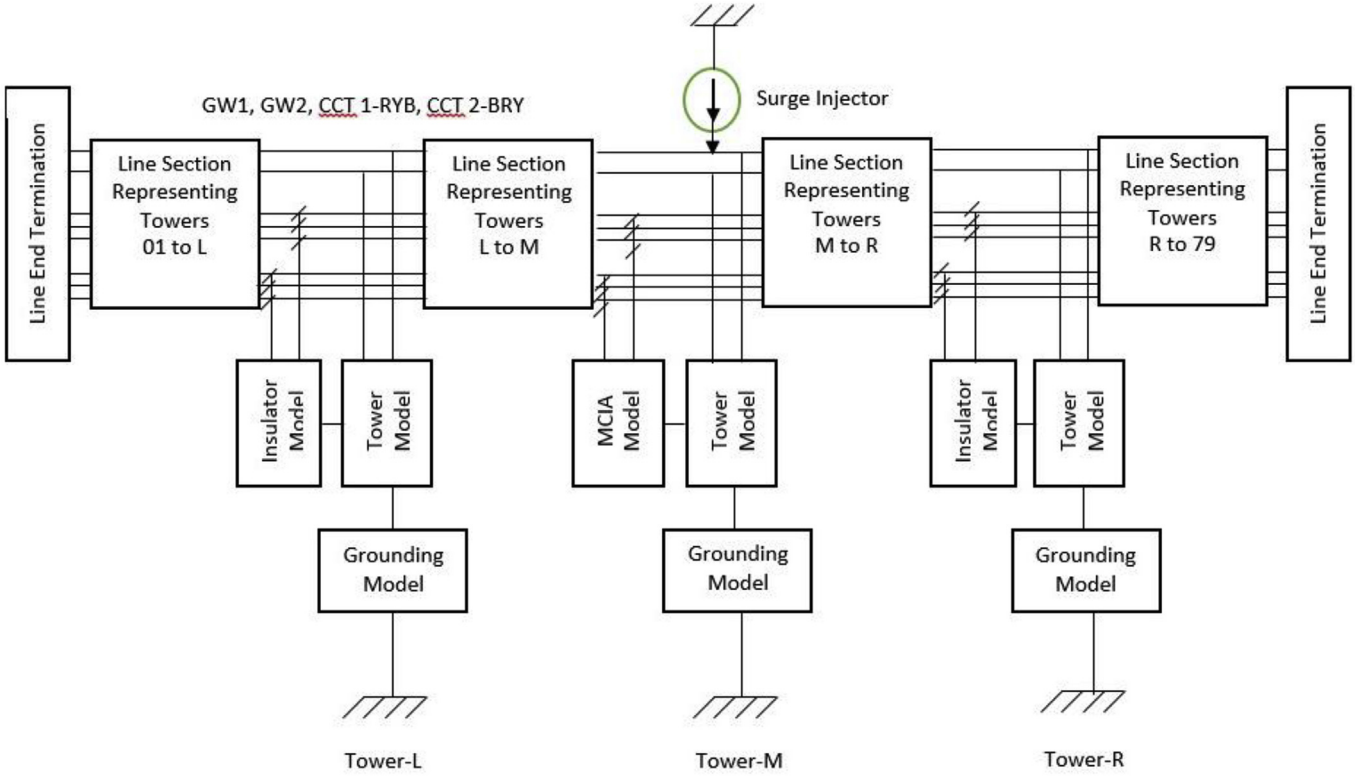

Fig. 3. Complete transmission line model for analysis.

the conductor. The main objective of this study is to investigate the feasibility of replacing conventional Insulator Strings with MCIA Strings.

Multi Chamber System (MCS) is the base design of the MCIA. It comprises of large number of electrodes mounted on the length of silicon rubber. The holes drilled between the electrodes that go through the length act as miniature gas discharge chambers. When a lightning overvoltage impulse is applied to the arrester, it breaks down the gaps between the electrodes. Discharges between electrodes occur inside chambers of a very small volume. The resulting high pressure drives spark discharge channels between electrodes to the surface of the insulating body and also into the air around the arrester. A blow-out action and an elongation of inter-electrode channels lead to an increase of the total resistance of all channels (i.e., that of the arrester), which limits the lightning overvoltage impulse current. Over recent years arc-quenching multi-chamber systems (MCS) are developed, succeeding in production of new 10–35 kV multi-chamber arresters (MCA), as well as a novel device termed "Multi Chamber Insulator Arrester (MCIA)" which combines the properties and functions of bit insulator and arrester. Fig. 2 illustrate a typical U120D glass MCIA.

To evaluate the feasibility of using MCIAs, the study is carried out in the following order:

a) Modeling of Multi Chamber Insulator Arrester (MCIA) for EMTP simulations and validations of the model.
b) Checking the performance for back-flashover effect of the transmission line of the MCIA installed system for pre-identified locations.
c) Calculation of the simple payback period for installation of MCIAs for pre-identified locations.

The following procedure is used in order to achieve the stated objectives:

a) Modeling and simulation of 132 kV Matugama-Kukule transmission line using PSCAD for lightning back-flashover analysis.
b) Modeling of MCIA for EMTP simulations and validations of the model.
c) Modeling and simulation of MCIA installed system (for pre-identified locations) in PSCAD for lightning back flashover analysis.
d) Conducting sensitivity analysis of MCIA line model for back-flashover effects.
e) Performance comparison between existing transmission line with the MCIA installed system.

3. Methodology

3.1. EMTP/PSCAD modeling and simulation

Electromagnetic Transient Programs is conveniently employed for analyzing the effects of lightning including back-flashovers of power transmission lines consisting fast front transients. The power transmission line and the back-flashover event are modeled using frequency dependent fast front transient models due to the presence of high frequency components in lightning strokes, typically ranging from 1 kHz to 30 MHz.

3.2. Proposed electromagnetic transient model for Kukule-Matugama transmission line

The basic hypothetical fast front transient transmission line model is developed using PSCAD Software as shown in Fig. 3. The complete line model consists of several sub-models representing the following transmission line elements.

a) "Transmission line section models" including towers up to the line end terminations (Ex: line section with towers from tower no.01 to L1 as shown in Fig. 3)
b) "Transmission line span models" between consecutive towers under study (Ex: span between tower no. L1 to M as shown in Fig. 3).

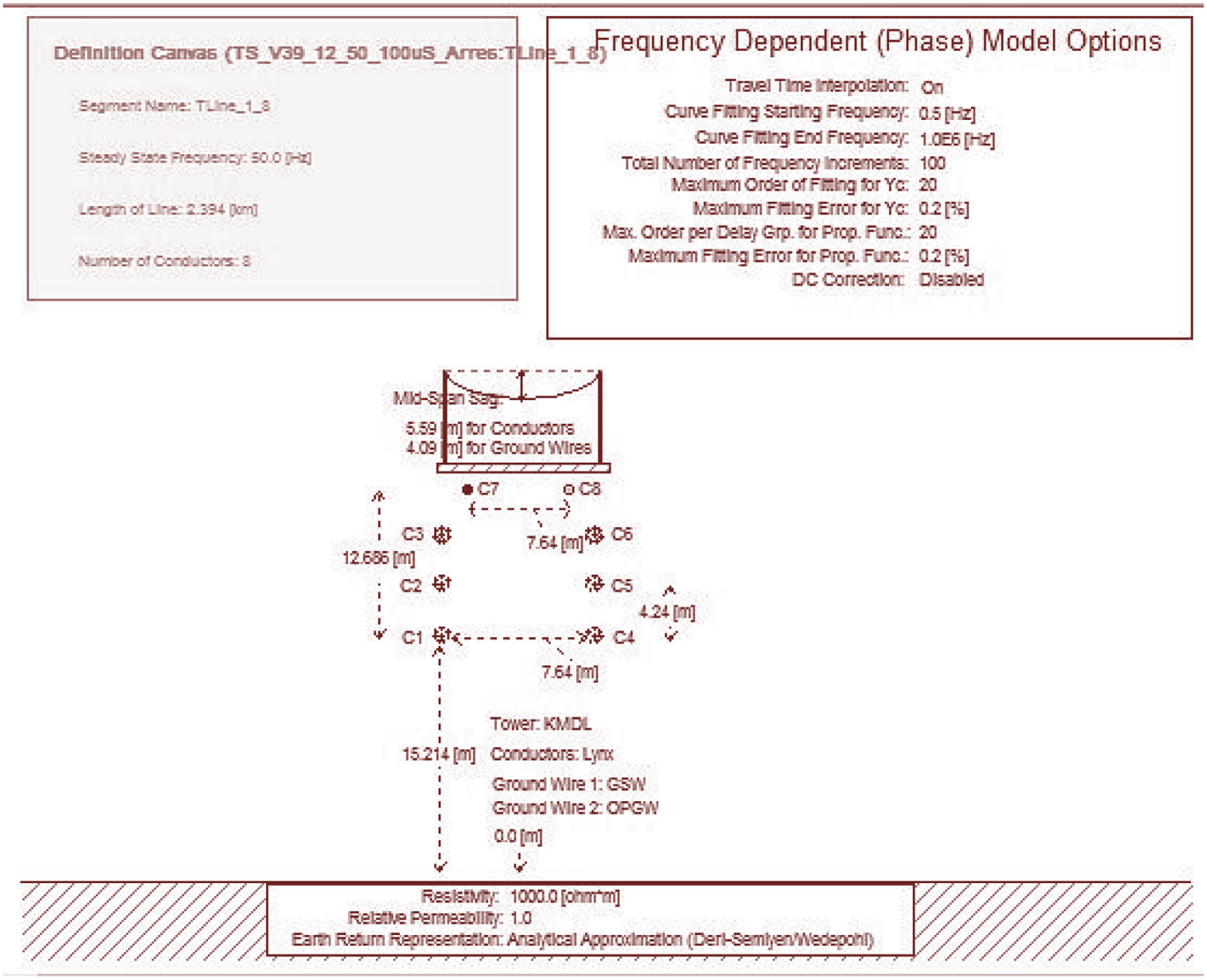

Fig. 4. General line Geometry data input.

c) Transmission tower model
d) Tower grounding resistance model
e) Line insulator string with back flashover model
f) Line end termination model
g) Surge Arrester model
h) Lightning surge generator model
i) Power frequency phase voltage generator model

As shown in Fig. 3, the complete line model consists of three towers named as M, L1 and R1. Tower M represent a typical tower with two adjacent towers L1 and R1 on the left and right sides respectively. The two line spans between these three towers are represented by the "line span models" whereas the rest of the line sections at each side up to the end terminations are represented by "line section models". Six numbers of interconnecting lines are used to connect each module while representing the ground and phase conductors from top to bottom sequence as shown in Fig. 3. All three tower models are connected to the Ground Wire- 1(GW-1) and Ground Wire-2 (GW-2) whereas the connections to the phase conductors are made through the insulator models. The surge generator (Current source) is always connected to the top of the middle tower.

3.2.1. *Transmission line model*

The transmission line sections and line spans are modeled using the standard frequency dependent phase model available in the Master Library of the PSCAD. There are two basic ways of constructing a transmission line in PSCAD by using the standard model and in this study the remote end method shown in Fig. 4 is used.

3.2.2. *Transmission tower model*

The transmission towers are modeled by the Constant Parameter Distributed Line (CPDL) model which consists of four (04) numbers of impedances in series with four numbers of parallel Resistance-Inductance branches as shown in Fig. 5. The tower model is created completely by using two basic passive components named resistor and inductor available in the Master Library of the PSCAD.

3.2.3. *Tower grounding resistance model*

A variable resistance component available in the PSCAD Master Library is used to represent the impulse grounding resistance of a transmission tower. The value of the variable resistance is varied externally by the "Multiple Run" simulation component. Fig. 6 shows a typical impulse grounding resistance model of a tower which is created with the aid of a variable resistor component in PSCAD.

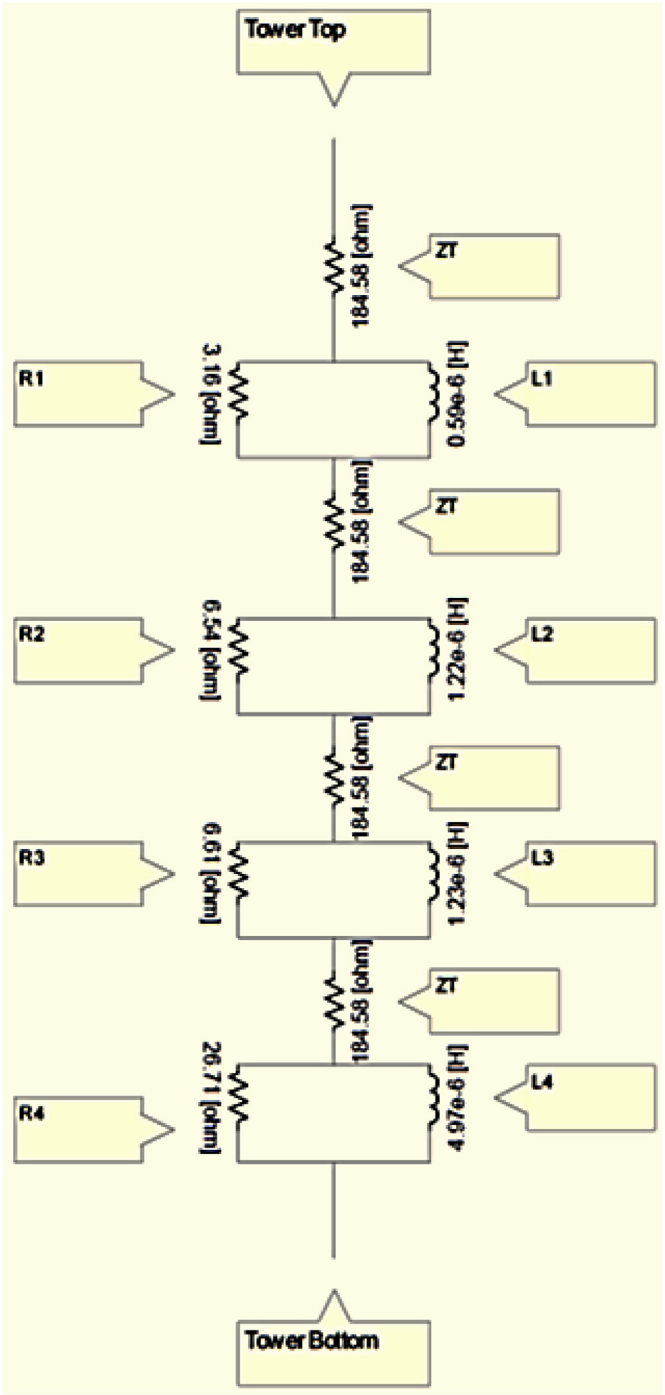

Fig. 5. Typical Tower Model created in PSCAD.

3.2.4. *Line insulator string with back-flashover model*

In lightning related calculations the estimated results are model dependent, especially if Volt-time curve as insulator strings flashover model is applied (Banjanin and Savic, 2016). Considering this, the insulator string and the back-flashover event are modeled by an equivalent capacitor in parallel with an externally controlled circuit breaker as shown in Fig. 7. The operation of circuit breaker is controlled by a back-flashover control module using basic control blocks available in the Master Library. The basic logic diagram for this is shown in Fig. 8.

This characteristic variation of flashover voltage of an insulator string can be modeled by a simplified expression given in (1).

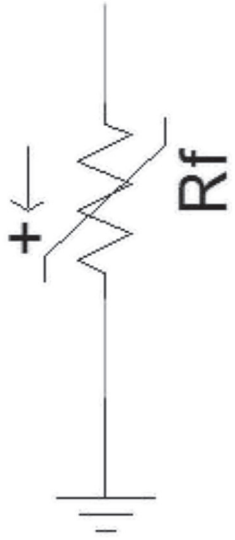

Fig. 6. Tower grounding resistance model.

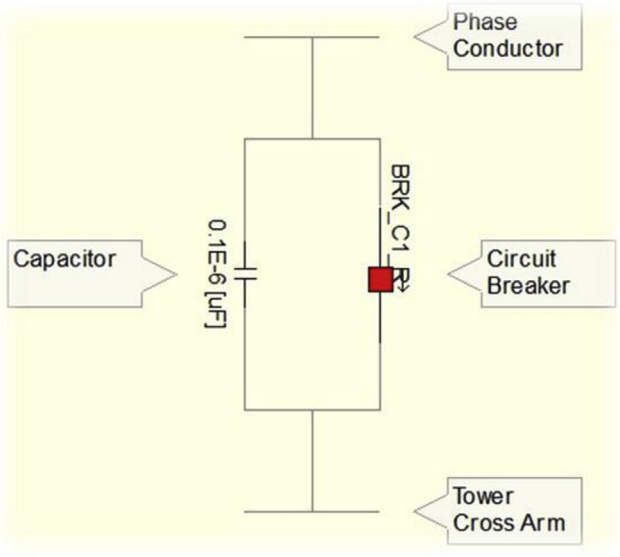

Fig. 7. Insulator string capacitor and back flashover breaker model.

$$V_{f0} = K_1 + \frac{K_2}{t^{0.75}} \quad (1)$$

where.

V_{f0} is the flashover voltage (kV)
$K_1 = 400 \times A_g$
$K_2 = 710 \times A_g$
A_g is the Arc-horn gap length (m)
t is the elapsed time after lightning stroke (μs)

Insulator String Voltage (V_{string}), Line to Ground Voltage (V_{line}), Arc Horn Gap length (=1.5 m) and Instantaneous Phase Voltage (V_a) are taken as the input data for the back-flashover control module. Inbuilt voltmeter components and their output signals are used to read the insulator string voltage and line to ground voltage whereas the instantaneous phase voltages are given by the power frequency phase voltage generator model.

The control components forming the left most branch of the module is

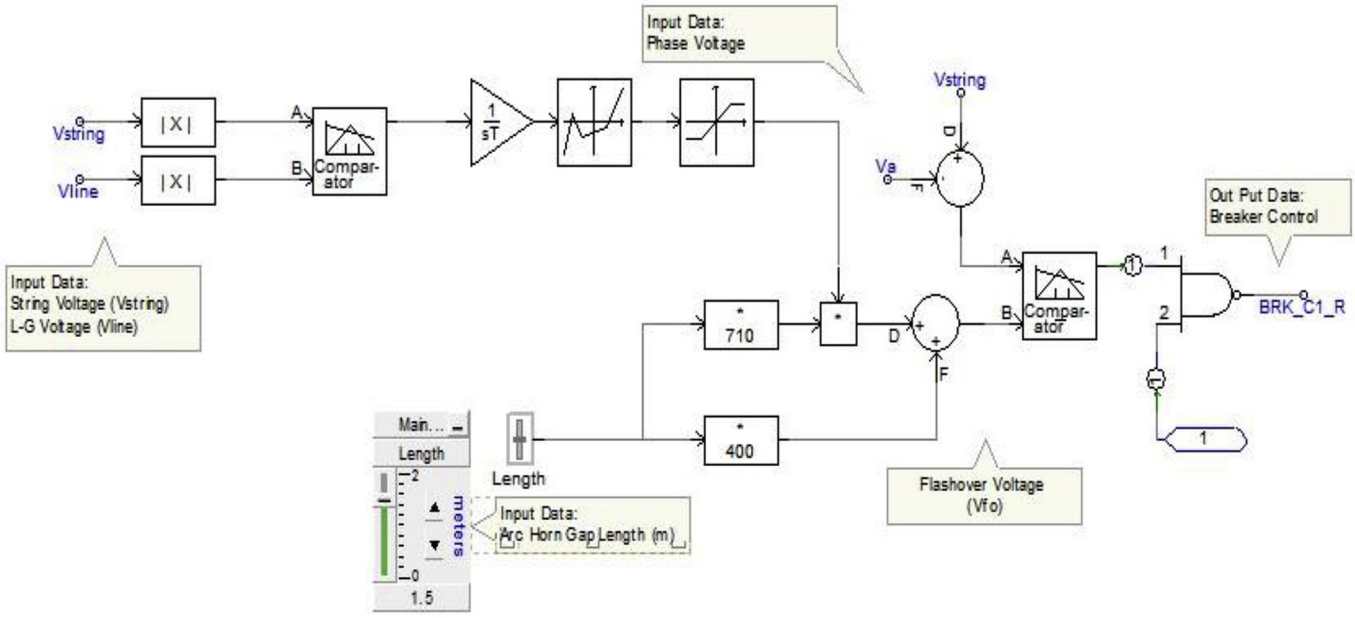

Fig. 8. Back-Flashover Control Module for conventional insulator string.

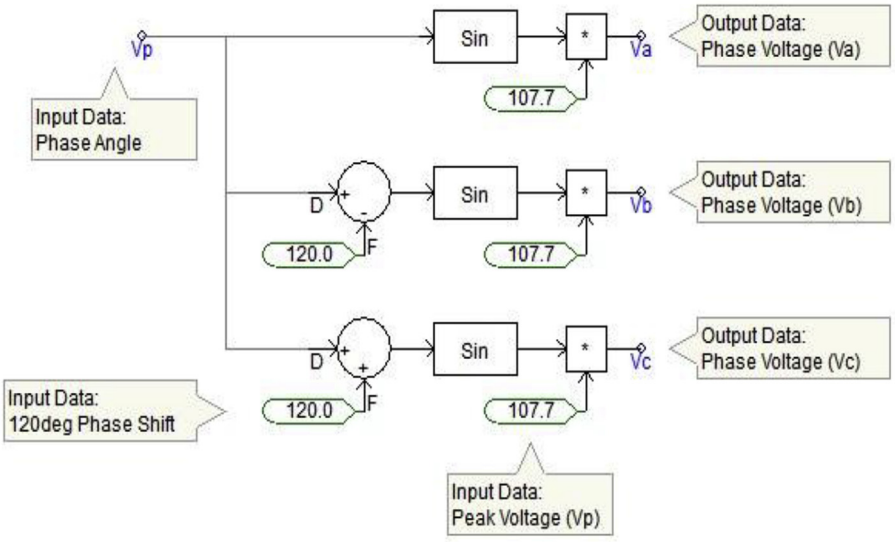

Fig. 9. Power frequency phase voltage generator model.

shown in Fig. 8 and is used in calculating the value ($1/t^{0.75}$) based on the input data V_{string} and V_{line}. The control components forming the loop, generates the flashover voltage value (V_{fo}) taking the arc horn gap length ($A_g = 1.5$ m) and the value ($1/t^{0.75}$) as the input parameters. The actual insulator string voltage is generated by the upper most differencing junction component taking the relevant power frequency phase voltage value and the measured string voltage as the input data. Finally the comparator component compares the generated V_{fo} and actual string voltage values. It gives the output signal as a positive pulse whenever the voltage profiles crosses each other which formulate a back-flashover event. Mono-stable component at the right most side of the model generates a digital output value "1" based on the positive pulse generated by the comparator component. Inverter component at the end of the model generates the digital value "0" required as an input data to the relevant circuit breaker to close the circuit. The close operation of the circuit breaker creates an external conductive path across the insulator string which simulates the back-flashover arc generated across the arc horn gaps.

3.2.5. *Power frequency phase voltage generator model*

The instantaneous power frequency phase voltages are generated using the circuit created in PSCAD shown in Fig. 9. The circuit is created for each phase voltage variation. The basic control components such as summing/differencing junctions, real/integer constants, trigonometric sine function and multipliers are used to create the circuit. The "phase angle" input data values are given by "Multiple Run" simulation component. The output phase voltages namely V_a, V_b and V_c are directly used in the back-flashover control modules to generate the actual insulator string voltages.

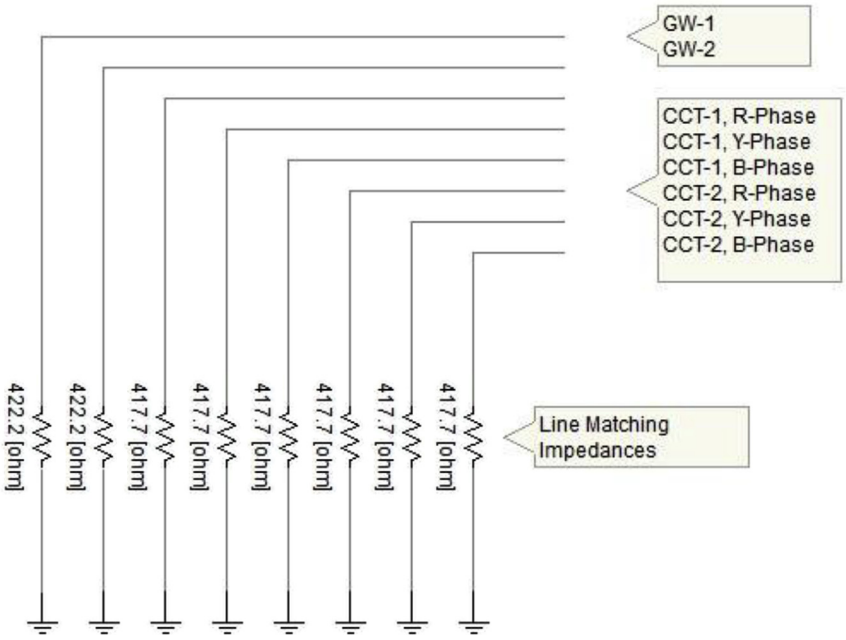

Fig. 10. Line Termination model created in PSCAD.

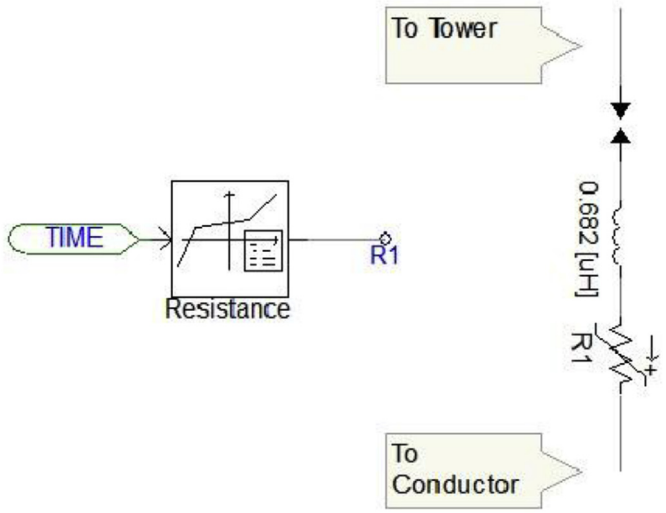

Fig. 11. MCIA model created in PSCAD.

Table 1
Properties of the X-Y transfer function.

Property	Value
X axis offset	0.0
Y axis offset	0.0
X axis gain	5.0
Y axis gain	1.0
Output mode	Interpolate
Periodic	No
Data entry method	File
Input Type	Real

3.2.6. *Line end termination model*

Two ends of the transmission line are grounded through equivalent surge impedances of each ground and phase conductors as shown in Fig. 10. Each end of the grounded impedances is connected to the nearest interfacing component of the transmission line section as per the relevant connection arrangement. The top two terminals of the interfacing component represent the two ground wires and the remaining six terminals represent the phase conductors of each circuit. The phase conductors of both circuits are grounded through 417.7 Ω equivalent impedances and similarly the ground conductors are grounded through 422.2 Ω equivalent impedances.

Table 2
Properties of spark gap.

Property	Value
Breakdown Voltage	625.0 [kV]
ON Resistance	0 [Ω]
OFF Resistance	1e6 [Ω]

3.2.7. *Multi Chamber Insulator Arrester model and the Back Flashover Control Module*

3.2.7.1. Multi Chamber Insulator Arrester (MCIA) model. The MCIA string with 10 numbers of insulators is modeled with an arc inductance in series with the ohmic resistance of its actuation as illustrated in Fig. 11. The calculated arc inductance is 0.682 μH and the ohmic resistance at actuation is fed to the variable resistor using the X-Y Transfer Function in the PSCAD Master Library. 120 data points are extracted and are used in the external file link option available in the X-Y transfer function to model the ohmic resistance of MCIA's actuation. Table 1 illustrates the properties of the X-Y transfer function and the X-Axis gain is set to "5".

The 50% impulse flashover voltage for MCIA with 10 numbers of insulators is 625 kV and to model this property for the MCIA model, the external spark gap is used in series with the arc inductance and ohmic resistance. Table 2 shows the properties window for the spark gap. The I-t and V-I graphs are obtained from PSCAD as indicated in Figs. 12 and 13 respectively. The output resembles the MCIA behavior and hence the developed model is validated.

3.2.7.2. Back Flashover Control Module for MCIA. The logic diagram for the back-flashover control module is implemented in PSCAD as shown in Fig. 14 by using basic control blocks available in the Master Library.

The control components forming the left upper most branch of the

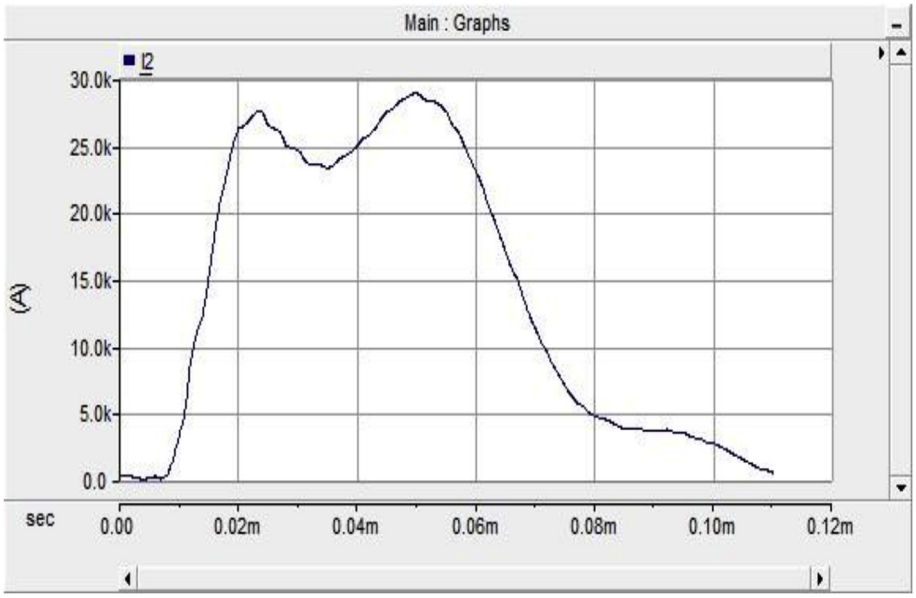

Fig. 12. MCIA model current variation with time.

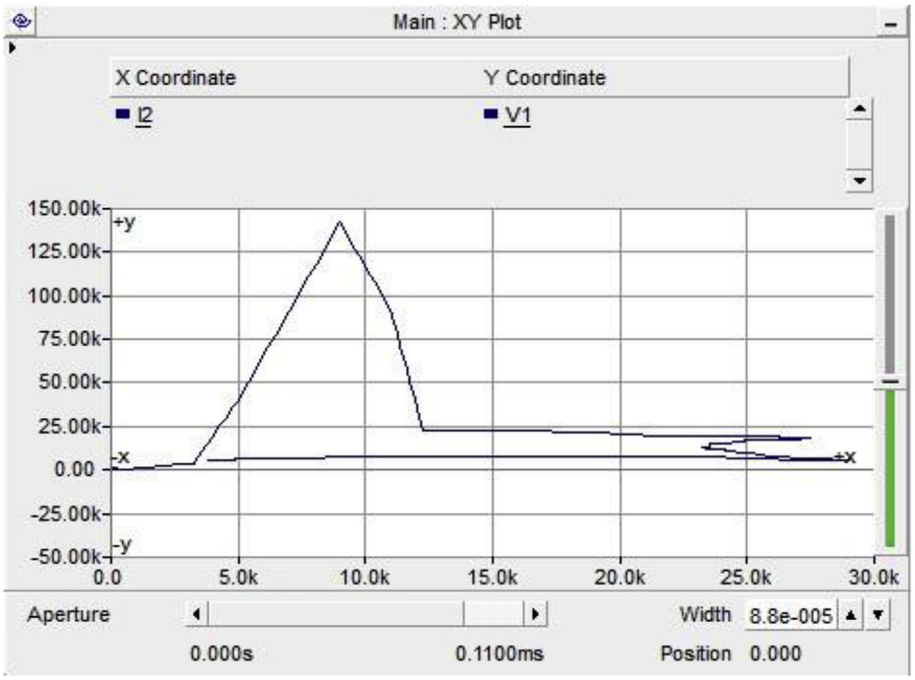

Fig. 13. MCIA model residual voltage variation with current.

module as shown in Fig. 14, calculates the value $t^{-0.544}$ based on the input data V_{string} and V_{line}. The control components forming the loop, generates the flashover voltage value (V_{fo}) taking the magnitude component (763.37) and the $t^{-0.544}$ value as the input parameters. The actual MCIA string voltage generated by the bottom left most differencing junction component taking the relevant power frequency phase voltage value and the measured string voltage as input data. Finally the comparator component compares the generated V_{fo} and the actual string voltage values and gives the output signal as a positive pulse whenever the voltage profiles are crosses each other which formulate a back flashover event. The mono-stable component at the right most side of the model generates a digital output value "1" based on the positive pulse generated by the comparator component. The inverter component at the end of the model generate the opposite digital value "0" required as an input data to the relevant circuit breaker to close the circuit. The close operation of the circuit breaker creates an external conductive path across the MCIA string which simulates the back flashover arc generated through the MCS. The MCIA string and the back flashover event are modeled by an equivalent capacitor parallel with an externally controlled circuit breaker as shown in Fig. 15.

3.2.8. *Lightning surge generator model*

The standard 8/20 μs double exponential waveform is generated by an inbuilt current source whose magnitude is controlled by an external control circuit shown in Fig. 16. The external control circuit consists of two similar parallel branches with a common input parameter

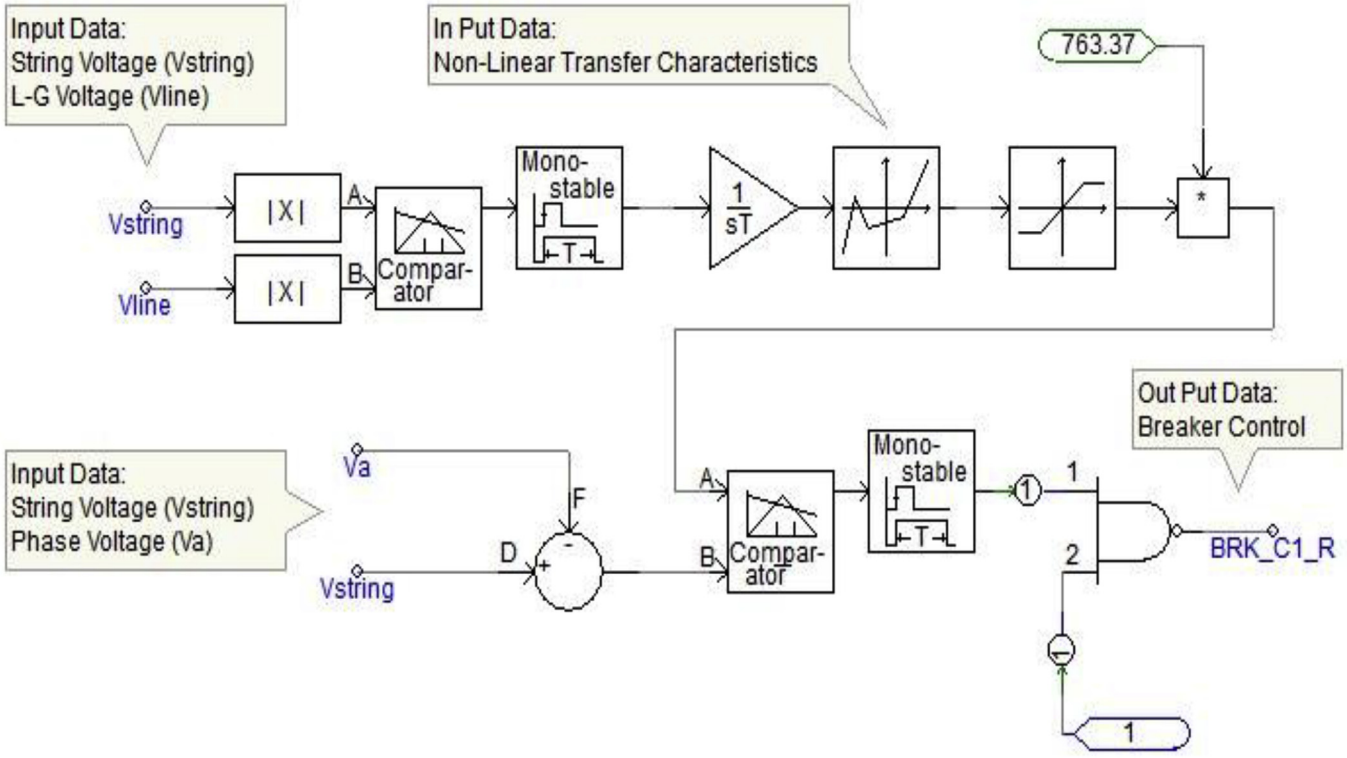

Fig. 14. Back Flashover Control Module for MCIA string implemented in PSCAD.

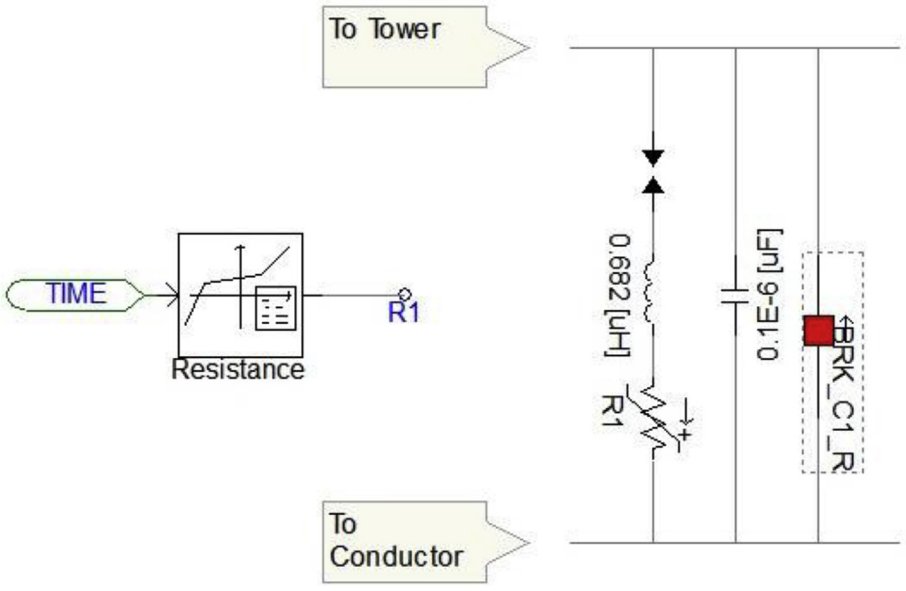

Fig. 15. MCIA string capacitor and back flashover breaker model.

component giving the simulation time of the system. Each branch consists of an exponential function component in series with a multiplier component. The multiplier component determines the magnitude of the current waveform which controlled externally by the "Multiple Run" simulation component. As shown in Fig. 16, the differencing junction component gives the instantaneous values of double exponential waveform to the current source. The current source generates the complete waveform based on the instantaneous values given by the control circuit. Fig. 17 shows the module output for 8/20μs surge waveform.

Similarly, a voltage source is used instead of the current source to generate the standard 1.2/50 μs voltage surge waveform and Fig. 18 shows the module output for 1.2/50 μs surge waveform. The interdependent sub-models such as back flashover model and phase voltage generator model are virtually interconnected by giving identical reference names for each common variable. For example, the "Phase Voltage" variable is referred to as V_a in both phase voltage generator model as well as in the back flashover model. During the same time frame, the phase voltage V_a is an output variable produced by the phase voltage generator model whereas it is an input to the back flash model. Similarly the data signals of the common variables are managed by assigning them with

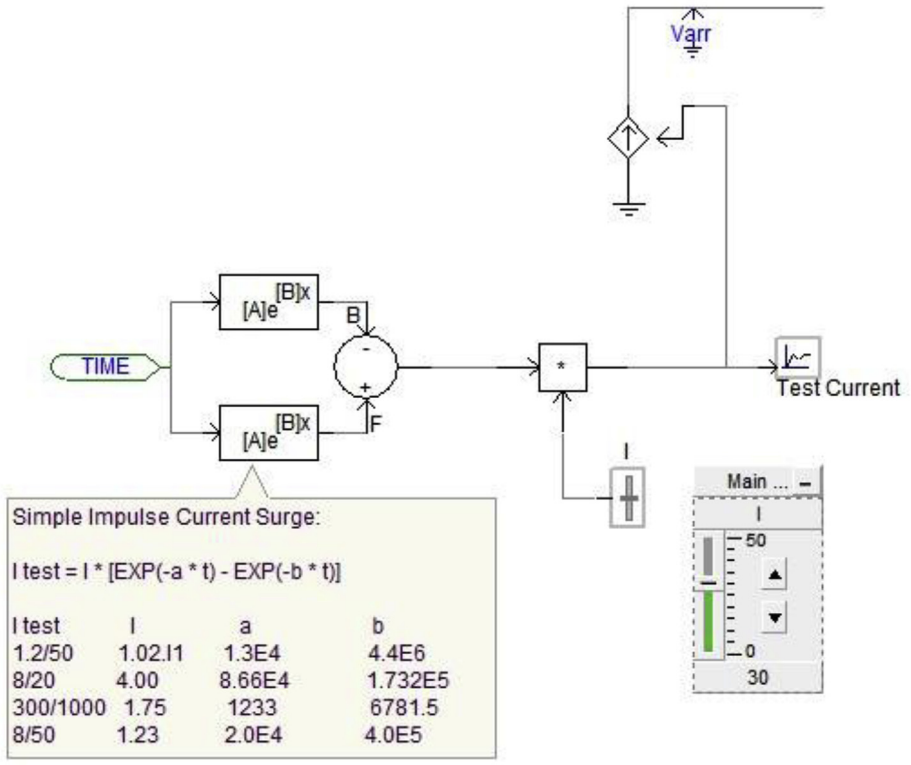

Fig. 16. Lightning Surge Generator Model created in PSCAD.

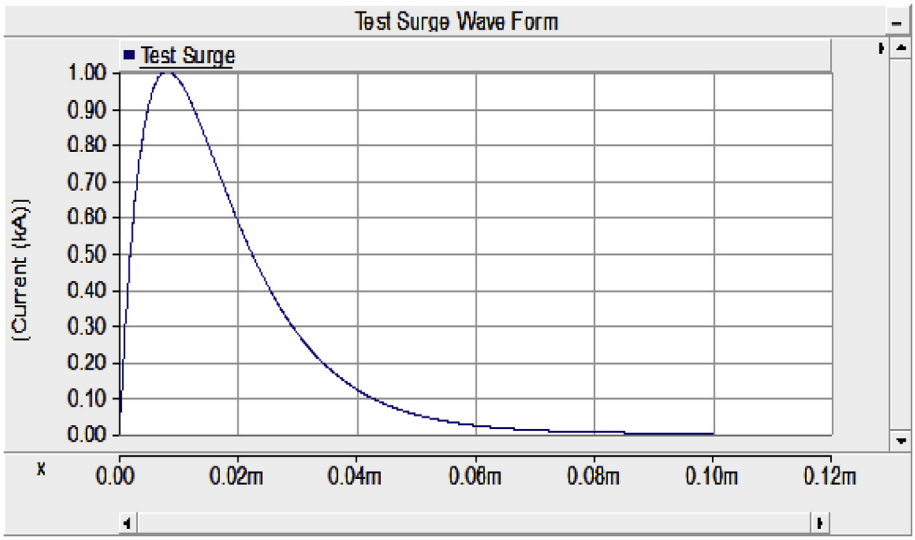

Fig. 17. 8/20 μs surge from the Created model.

identical data signal labels.

3.3. Method of simulation

3.3.1. Multiple run component and variable settings

Simulation of the completed final transmission line model is carried out using the "Multiple Run" simulation component available in the Master Library of PSCAD as shown in Fig. 19. This component is used to control a multiple run, while manipulating variables from one run to the next. These variables are output from the component (up to six outputs) and may be connected to any other PSCAD components. The Multiple Run component also records up to six channels per run.

Three numbers of variables those directly affecting the back flash-overs are varied in each run of the simulation by using the Multiple Run component. The three variables are:

a) Magnitude of the lightning surge current labeled as "I" in the model is set as V1 of Multiple Run component.
b) Phase angle of the power frequency phase voltage labeled as "Ph" in the model is set as V2 of Multiple Run component 3.
c) Grounding resistance of Tower-M labeled as "Rf" in the model is set as V3 of Multiple Run component.

The range of values set for each variable in the Multiple Run

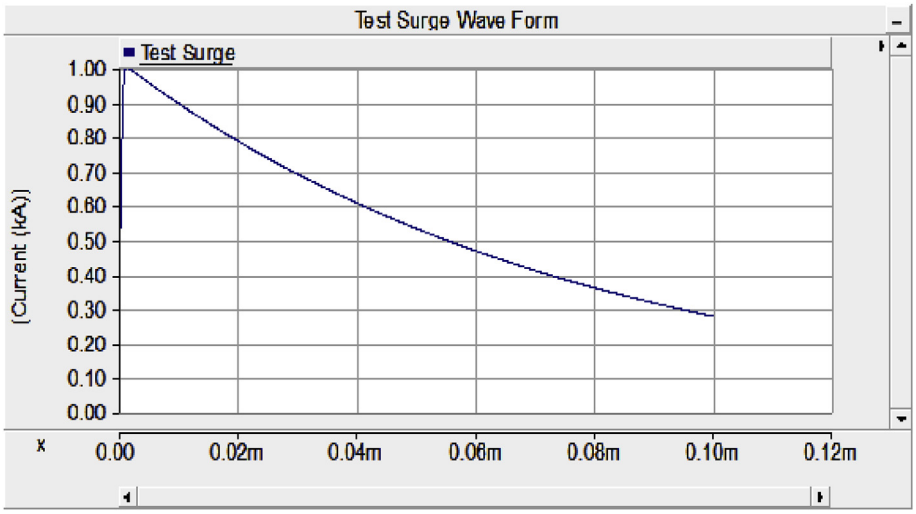

Fig. 18. 1.2/50 μs surge from the Created model.

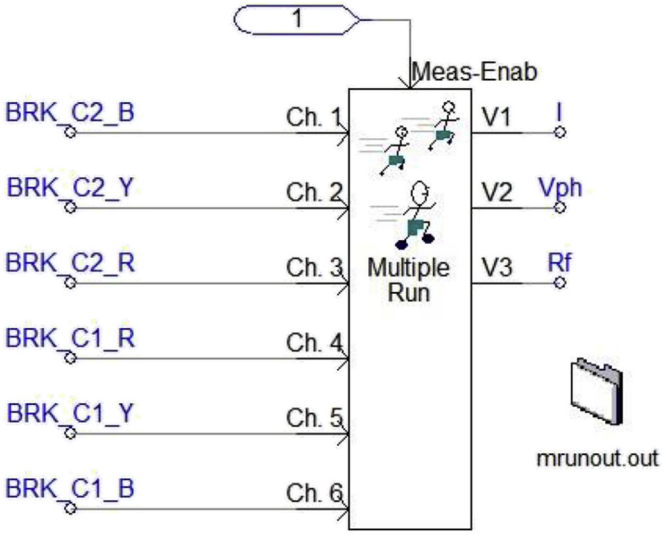

Fig. 19. Multiple-Run Simulation component of PSCAD.

Table 4
Simulation criteria for step-1.
Step 2 Simulation of the model with arrester protection.

Simulation number	Surge waveform	Tower grounding resistance (Ω)	Expected phases where the control signal output data to be recorded
01	8 × 20 μs	9	Tower-M, Circuit-1and Circuit-2 All six (06) phases
02	8 × 20 μs	38	Tower-M, Circuit-1and Circuit-2 All six (06) phases
03	8 × 20 μs	146	Tower-M, Circuit-1and Circuit-2 All six (06) phases
04	1.2 × 50 μs	9	Tower-M, Circuit-1and Circuit-2 All six (06) phases
05	1.2 × 50 μs	38	Tower-M, Circuit-1and Circuit-2 All six (06) phases
06	1.2 × 50 μs	146	Tower-M, Circuit-1and Circuit-2 All six (06) phases

Table 3
Range of values used for variables in Multiple-Run component.

Variable in Multiple Run component	Data label used in the model	Range of values
V1	I	20 kA–200 kA with 10 kA steps
V2	Ph	0° to 360° with 10° steps
V3	Rf	38 Ω, 146 Ω, 9 Ω

component is shown in Table 3.

The shielding failure flashovers were more frequent at surge current values less than 20 kA; whereas the back flashovers take place at higher surge current ratings of around 80 kA. Therefore a range of values from 20 kA to 200 kA with 10 kA step is selected for the variable "I" as shown in Table 3. Simulations are carried out from 0° to 360° full range of phase angles with a 10° phase angle step to examine the effect of phase angle on back-flashovers. The grounding resistance of the Tower-M is set to one of the three values in each simulation as shown in Table 3. As observed, the recorded maximum tower grounding resistance even with the soil ionization effect is approximately 38 Ω when the surge current is about 30 kA. Therefore, the value 38 Ω is the recorded worst case of tower grounding resistance with the soil ionization effect and is selected as one of the three values used in the simulations. It is also observed that the maximum recorded tower grounding resistance is approximately 146 Ω when the soil ionization effect is not considered. Therefore, the value 146 Ω is taken as the worst case of tower grounding resistance when the soil ionization effect is neglected. Therefore the value 146 Ω is also selected as the second value to be used in the simulations as tower grounding resistance variable V3 as shown in Table 3. The standard value specified by the local utility for the tower grounding resistance of any transmission line is approximately 10 Ω. Therefore, a value less than 10 Ω (assume 9 Ω) is used in the simulations to investigate the performance of towers against lightning back-flashovers. While changing the value of above variables in each run of the simulations, the control signal output of each back-flashover control modules are recorded with the aid of six channel recorders available in the same Multiple Run component. The recorded control signal outputs are stored in an output file assigned to the Multiple Run component. These control signal output data are in binary form where the output "0" represents a back-flashover event.

Table 5
Simulation criteria for step-2.

Simulation number	Surge waveform	Tower grounding resistance (Ω)	Expected phases where the control signal output data to be recorded
With 02 arresters installed at TOP phase of Circuit-1and Circuit-2 of Tower-M			
07	8 × 20 μs	9	Tower-M, Circuit-1and Circuit-2 All six (06) phases
08	8 × 20 μs	38	Tower-M, Circuit-1and Circuit-2 All six (06) phases
09	8 × 20 μs	146	Tower-M, Circuit-1and Circuit-2 All six (06) phases
10	1.2 × 50 μs	9	Tower-M, Circuit-1and Circuit-2 All six (06) phases
11	1.2 × 50 μs	38	Tower-M, Circuit-1and Circuit-2 All six (06) phases
12	1.2 × 50 μs	146	Tower-M, Circuit-1and Circuit-2 All six (06) phases
With 04 arresters installed at TOP and MIDDLE phases of Circuit-1and Circuit-2 of Tower-M			
13	8 × 20 μs	9	Tower-M, Circuit-1and Circuit-2 All six (06) phases
14	8 × 20 μs	38	Tower-M, Circuit-1and Circuit-2 All six (06) phases
15	8 × 20 μs	146	Tower-M, Circuit-1and Circuit-2 All six (06) phases
16	1.2 × 50 μs	9	Tower-M, Circuit-1and Circuit-2 All six (06) phases
17	1.2 × 50 μs	38	Tower-M, Circuit-1and Circuit-2 All six (06) phases
18	1.2 × 50 μs	146	Tower-M, Circuit-1and Circuit-2 All six (06) phases
With 06 arresters installed on all the phases of Circuit-1and Circuit-2 of Tower-M			
19	8 × 20 μs	9	Tower-M, Circuit-1and Circuit-2 All six (06) phases
20	8 × 20 μs	38	Tower-M, Circuit-1and Circuit-2 All six (06) phases
21	8 × 20 μs	146	Tower-M, Circuit-1and Circuit-2 All six (06) phases
22	1.2 × 50 μs	9	Tower-M, Circuit-1and Circuit-2 All six (06) phases
23	1.2 × 50 μs	38	Tower-M, Circuit-1and Circuit-2 All six (06) phases
24	1.2 × 50 μs	146	Tower-M, Circuit-1and Circuit-2 All six (06) phases
25	8 × 20 μs	9	Tower-L, Circuit-1and Circuit-2 All six (06) phases
26	8 × 20 μs	38	Tower-L, Circuit-1and Circuit-2 All six (06) phases
27	8 × 20 μs	146	Tower-L, Circuit-1and Circuit-2 All six (06) phases
28	1.2 × 50 μs	9	Tower-L, Circuit-1and Circuit-2 All six (06) phases
29	1.2 × 50 μs	38	Tower-L, Circuit-1and Circuit-2 All six (06) phases
30	1.2 × 50 μs	146	Tower-L, Circuit-1and Circuit-2 All six (06) phases
31	8 × 20 μs	9	Tower-R, Circuit-1and Circuit-2 All six (06) phases
32	8 × 20 μs	38	Tower-R, Circuit-1and Circuit-2 All six (06) phases
33	8 × 20 μs	146	Tower-R, Circuit-1and Circuit-2 All six (06) phases
34	1.2 × 50 μs	9	Tower-R, Circuit-1and Circuit-2 All six (06) phases
35	1.2 × 50 μs	38	Tower-R, Circuit-1and Circuit-2 All six (06) phases
36	1.2 × 50 μs	146	Tower-R, Circuit-1and Circuit-2 All six (06) phases

4. Results and discussion

4.1. Simulation criteria

The simulation of the complete line model is carried out in two steps. In the first step, the model is simulated without MCIA for selected three (03) critical tower grounding resistance values 9 Ω, 38 Ω and 146 Ω for both 8 × 20 μs and 1.2 × 50 μs surge waveforms. In the second step, the model is simulated with the MCIA in three different arrester configurations for both 8 × 20 μs and 1.2 × 50 μs surge waveforms. For all simulations the lightning surge current is injected at the top of the Tower M. The detailed criteria of each simulation including the tower grounding resistance setting and expected control signal output data to be recorded are described in Tables 4 and 5.

mrunout.out - Notepad

File Edit Format View Help

Multiple Run Output File

Run #	I	Vph	Rf	BRK_C2_B	BRK_C2_Y	BRK_C2_R	BRK_C1_R	BRK_C1_Y	BRK_C1_B
1	20	0	9	1	1	1	1	1	1
2	30	0	9	1	1	1	1	1	1
3	40	0	9	1	1	1	1	1	1
4	50	0	9	1	1	1	1	1	1
5	60	0	9	1	1	1	1	1	1
6	70	0	9	1	1	1	1	1	1
7	80	0	9	1	1	1	1	1	1
8	90	0	9	1	1	1	1	1	1
9	100	0	9	1	1	1	1	1	1
10	110	0	9	1	1	1	1	1	1
11	120	0	9	1	1	1	1	1	1
12	130	0	9	1	1	0	1	1	0
13	140	0	9	1	1	0	1	1	0
14	150	0	9	1	1	0	1	1	0
15	160	0	9	1	0	1	1	0	1
16	170	0	9	1	0	1	1	0	1
17	180	0	9	1	0	1	1	0	1
18	190	0	9	1	0	1	1	0	1
19	200	0	9	1	0	1	1	0	1
20	20	10	9	1	1	1	1	1	1
21	30	10	9	1	1	1	1	1	1
22	40	10	9	1	1	1	1	1	1
23	50	10	9	1	1	1	1	1	1
24	60	10	9	1	1	1	1	1	1
25	70	10	9	1	1	1	1	1	1
26	80	10	9	1	1	1	1	1	1
27	90	10	9	1	1	1	1	1	1
28	100	10	9	1	1	1	1	1	1
29	110	10	9	1	1	1	1	1	1
30	120	10	9	1	1	1	1	1	1
31	130	10	9	1	1	0	1	1	0
32	140	10	9	1	1	0	1	1	0
33	150	10	9	1	1	0	1	1	0
34	160	10	9	1	0	1	1	0	1

Fig. 20. Typical view of an output data file.

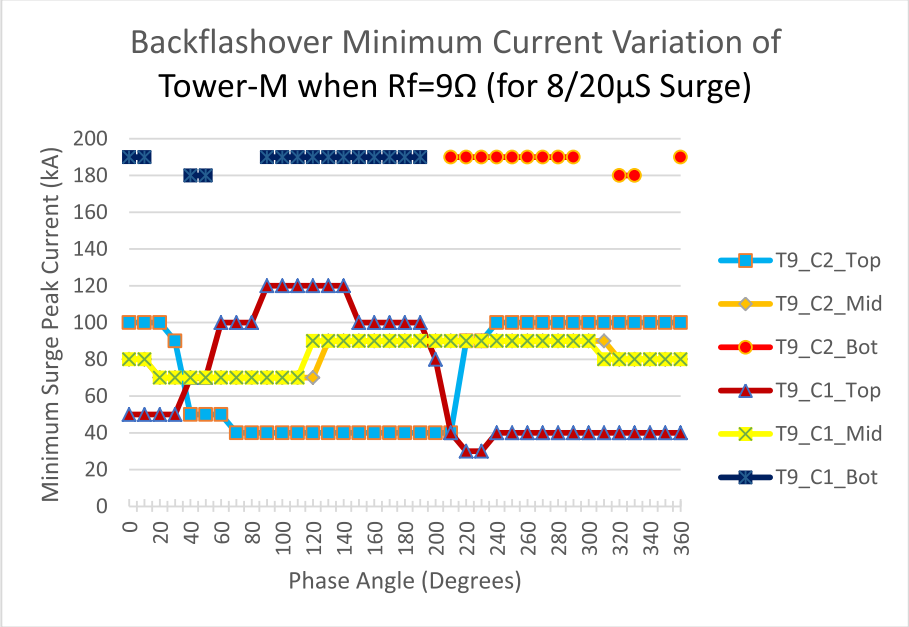

Fig. 21. Simulation results with no MCIA protection for 8/20 μS Surge for the ground resistance of 9 Ω

4.2. Project simulation settings

The simulation settings are assigned for each simulation run as follows:

1. Duration of each run = 200 μs
2. Solution time step = 0.1 μs
3. Channel plot step = 0.1 μs

Step 1 Simulation of the model without arrester protection.

4.3. Technical analysis

4.3.1. Introduction to simulation results

The results of each simulation are given by an output data file which contains a set of binary values giving the occurrence of back flashover events for each simulation run. The binary value "0" means an

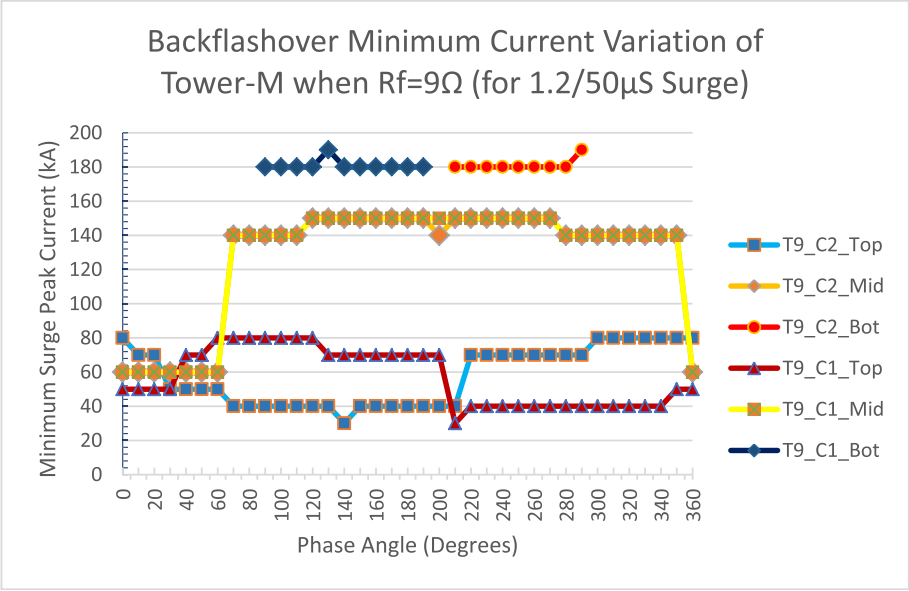

Fig. 22. Simulation results with no MCIA protection for 1.2/50 μS Surge for the ground resistance of 9 Ω

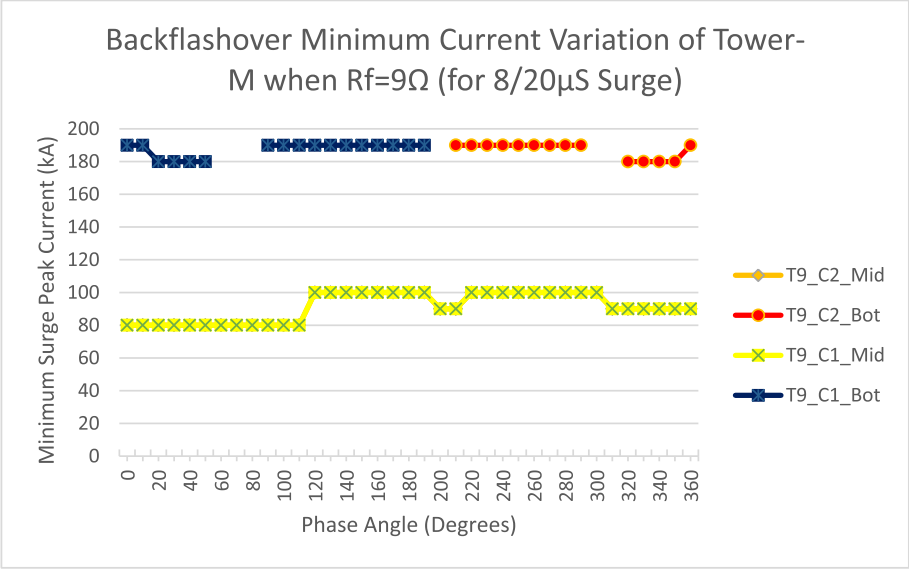

Fig. 23. Simulation results with two MCIA protection on TOP phases for 8/20 μS Surge for the ground resistance of 9 Ω

occurrence of a back flashover event whereas "1" gives the negation of that event. A typical view of an output data file is shown in Fig. 20.

The columns BRK_C2_B, BRK_C2_Y and BRK_C2_R indicate the occurrence of back flashover events on TOP, MIDDLE and BOTTOM phases of Circuit-2 of Tower-M respectively. Similarly the columns BRK_C1_R, BRK_C1_Y and BRK_C1_B indicate the occurrence of back flashover events on TOP, MIDDLE and BOTTOM phases of Circuit-1 of Tower-M respectively. Based on the information provided by the output files of each simulation, the variation of minimum current required for back-flashover event are produced and plotted as the final results.

4.3.2. Back flashover minimum current variation results and analysis

4.3.2.1. Results of simulations without MCIA protection (Step-1). Step 1 consists of six numbers of simulations from simulation no-01 to 06. All these six numbers of simulations were carried out without MCIA module for both 8 × 20 μs and 1.2 × 50 μs surge waveforms respectively. Further, above simulations are also done for selected 9 Ω, 38 Ω and 146 Ω tower grounding resistances values. As per the results shown in Fig. 21 (Step-1, Simulation No.01), it is evident that for the 8/20 μS surge, with a 9 Ω tower footing resistance, all the six phases of both circuits get back-flashover at different peak values of the surges. Among these peak values, the minimum peak currents for TOP, MIDDLE and BOTTOM phases are 40 kA, 70 kA and 180 kA respectively. A similar pattern, but with different peak values is observed for ground resistances of 38 Ω and 146 Ω.

For the 1.2/50 μS surge with a 9 Ω tower footing resistance shown in Fig. 22 (Step-1, Simulation No.04), all the six phases of both circuits gets back flashover at peak values of the surges different from the 8/20 μS surge and 9 Ω tower footing resistance. However, TOP phase flashover minimum peak surge current drops to 30 kA and for MIDDLE phases it is reduced to 60 kA when compared with 1.2/50 μS surge and for 9Ω tower footing resistance results. A similar pattern, with different peak values is witnessed for ground resistances of 38 Ω and 146 Ω. However, when

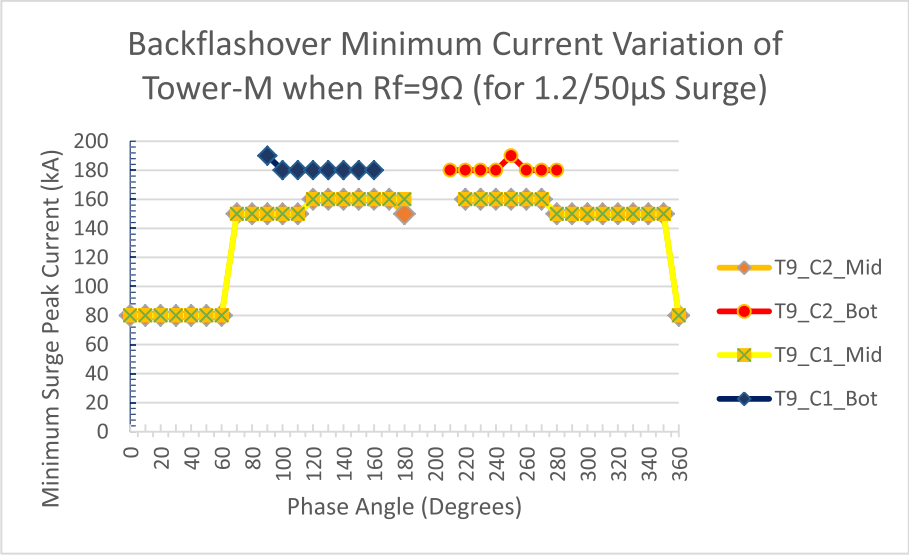

Fig. 24. Simulation results with two MCIA protection on TOP phases for 1.2/50 μS Surge for the ground resistance of 9Ω.

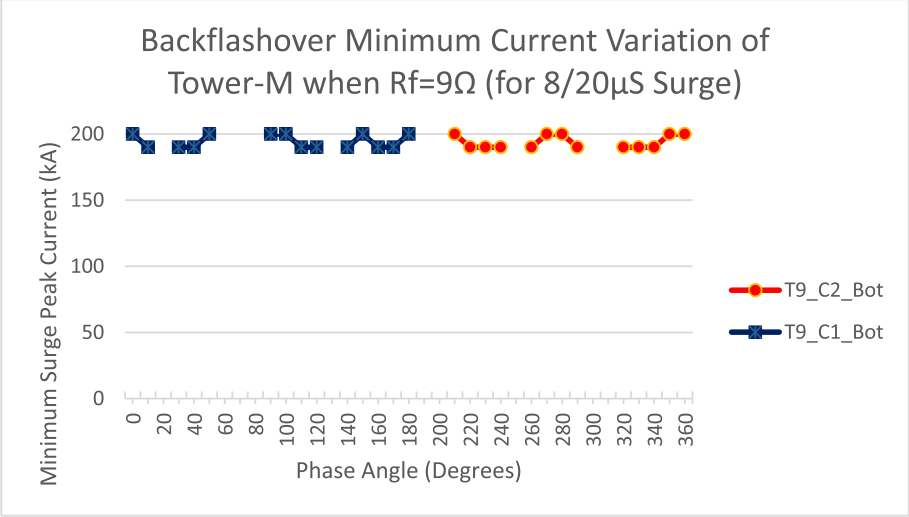

Fig. 25. Simulation results with Four MCIA protection on TOP and MIDDLE phases for 8/20 μS Surge for the ground resistance of 9Ω.

considering the behavior for 8/20 μS and 1.2/50 μS surges, it is seen that similar back flashover patterns are followed for different flashover minimum peak surge currents for ground resistances of 9 Ω, 38 Ω and 146 Ω. Also, it is concluded that there is no protection at all for back flashover up to 200 kA peak surge currents for any phases of the both circuits.

4.3.2.2. Results of simulations with MCIA protection (Step-2). With 02 MCIAs installed at TOP phase of Circuit-1and Circuit-2 of Tower-M.

When TOP phases of the Circuit 1 and 2 are replaced by the MCIA strings, it is clearly seen that the TOP phases are protected from the back flashover effect even up to 200 kA peak current surges for both 8/20 μS and 1.2/50 μS surges. However, MIDDLE and BOTTOM phases of both circuits get the impact of flashover for both 8/20 μS and 1.2/50 μS surges with different minimum peak surge current as seen in Figs. 23 and 24 for all ground resistance values.

The minimum peak surge current values when compared to the "no MCIA protection (Step-1, Simulations 1–6)" has increased in every simulations for "with MCIA protection for top phases". This is evident by comparing Fig. 21 with Figs. 23 and Fig. 22 with Fig. 24 respectively.

4.3.2.2.1. With 04 MCIA installed at TOP and MIDDLE phases of Circuit-1and Circuit-2 of Tower-M. From simulation no.13–18, the system was equipped with 04 Nos. of MCIA strings on TOP and MIDDLE phases of the both circuits. Fig. 25 shows the simulation results for 8/20 μS surge with tower footing resistance of 9Ω. From this it is evident that TOP and MIDDLE phases of both circuits have protection for back-flashover effect up to the 200 kA maximum peak surge current. However, BOTTOM phases of both circuits are not protected by the MCIA installed on TOP and MIDDLE phases of both circuits. But the minimum peak surge currents at which back flashover occur have increased significantly. This is same for the 1.2 × 50 μs surge as in Fig. 26 for all the grounding resistance values which clearly illustrates the behavior of 04 MCIA string protection systems for the 8 × 20 μs and 1.2 × 50 μs surges for 38 Ω and 146 Ω respectively.

4.3.2.2.2. With 06 MCIA installed on all the phases of Circuit-1and Circuit-2 of Tower-M.

- For 8 × 20 μs surge and for 9 Ω, 38 Ω and 146 Ω, there is no occurrence of back flashover event in all six phases of the Tower-M.

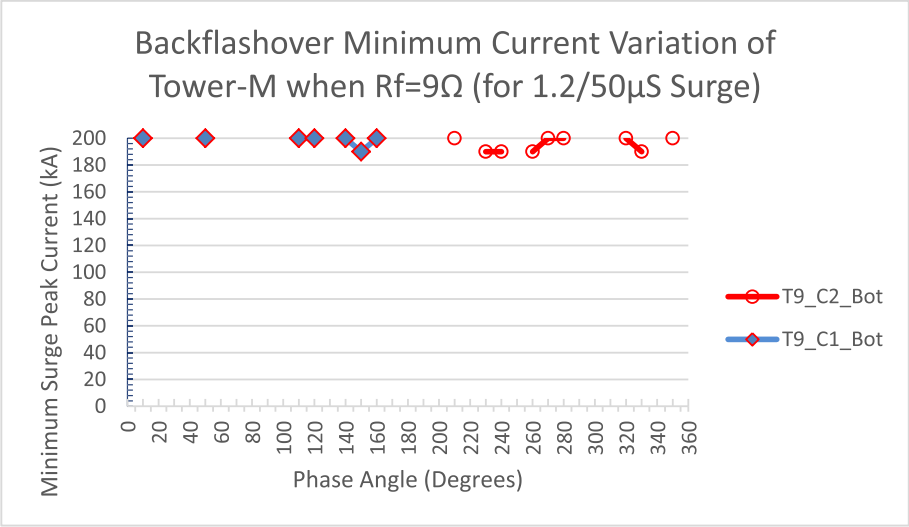

Fig. 26. Simulation results with Four MCIA protection on TOP and MIDDLE phases for 1.2/50 μS Surge for the ground resistance of 9 Ω

Table 6
Properties of the conventional insulator string and MCIA string.

No.	Description	Conventional Insulator	MCIA String	Remarks
01	Spacing	146 mm	146 mm	
02	Diameter	255 mm	413 mm	
03	No of Discs	11	10	
04	Creepage Distance (Per Unit)	320 mm	360 mm	
05	Creepage Distance (String)	3520 mm	3600 mm	
06	Weight	5 kg	6.7 kg	17 kg of excess load to the Cross arm and can be easily beard
07	Mechanical Strength	120 kN	120 kN	
08	String Length with Accessories	2106 mm (1606 + 500)	2106 mm (1606 + 646)	String Length can be adjusted with hardware accessories

- For 1.2 × 50 μs surge and for 9 Ω, 38 Ω and 146 Ω, there is no occurrence of back flashover event in all six phases of the Tower-M.
- For 8 × 20 μs surge and for 9 Ω, 38 Ω and 146 Ω, there is no occurrence of back flashover event in all six phases of the Tower-L.
- For 1.2 × 50 μs surge and for 9 Ω, 38 Ω and 146 Ω, there is no occurrence of back flashover event in all six phases of the Tower-L.
- For 8 × 20 μs surge and for 9 Ω, 38 Ω and 146 Ω, there is no occurrence of back flashover event in all six phases of the Tower-R.
- For 1.2 × 50 μs surge and for 9 Ω, 38 Ω and 146 Ω, there is no occurrence of back flashover event in all six phases of the Tower-R.

4.3.3. *Electrical and mechanical properties*

The electrical and mechanical properties of conventional insulator string and MCIA string is given in Table 6.

4.4. *Calculation of simple pay back period*

The period 2010–2014 is considered for calculation of the simple payback period. The calculations are carried out considering spilling and non-spilling conditions of the Kukule regulating pond. It is shown that the simple payback period (when the regulating pond is spilling) is 2.33 years when the loss of generation is substituted by coal power generation and it is 0.35 years when loss of generation is substituted by next lowest thermal generation, Sapugaskanda power station. It is witnessed that simple payback period (when the regulating pond is not spilling) is 3.5 years when loss of generation is substituted by the coal power generation and the substituted generation is sold to consumers who use less than 30 kWh per month. However, simple payback period is 0.37 years (when the regulating pond is not spilling) when loss of generation is substituted by the next lowest thermal generation, Sapugaskanda power station sold to consumers who use less than 30 kWh per month. Further, the simple payback period is 0.57 years when loss of generation is substituted by next lowest thermal generation, Sapugaskanda Power Station and the substituted generation is sold to consumers who use more than 60 kWh per month.

5. Conclusion

The reliability of a power system depends on the performance of transmission lines. The transmission line outages occur predominantly due to back flashover effects. This paper demonstrates the effectiveness of MCIAs in eliminating back-flashover effects. The 132 kV, Matugama-Kukle transmission line was modeled and simulated with and without MCIAs using PSCAD. This helped in identifying the right combination of MCIAs to be installed in all phases of the double circuit. It is recommended to replace all the conventional insulator strings with MCIA strings of the tower of interest where the most insulator damages are recorded and then, towers in the either sides of the interested tower are also protected for the back-flashover effect. Frequent inspections after installing MCIAs are recommended and subsequently the frequency of inspections may be adjusted based on the observed performance of the MCIA strings. The inspection of the Multi Chamber System (MCS) on the perimeter of the Insulator for any abnormalities and deformations is also recommended. If any abnormalities and deformations are observed, the respective MCIA should be replaced according to the practice used by the utility for changing insulators. Special care should be taken to avoid damages the MCS of MCIA.

Acknowledgments:

The authors gratefully acknowledge the support provided by the Senate Research Council, University of Moratuwa (SRC/LT/2015/04).

References

Andreotti, A., Pierno, A., Rakov, V.A., 2015. A new tool for calculation of lightning-induced voltages in power systems—Part I: development of circuit model. IEEE Trans. Power Del. 30 (1), 326–333.

Banjanin, M.S., 2018. Application possibilities of special lightning protection systems of overhead distribution and transmission lines. Int. J. Electr. Power Energy Syst. 10.

Banjanin, M.S., Savic, M.S., 2016. Some aspects of overhead transmission lines lightning performance estimation in engineering practice. Int. Trans. Electrical Energy Syst. 26 (1), 79–93.

Banjanin, M.S., Savić, M.S., Stojković, Z.M., 2015. Lightning protection of overhead transmission lines using external ground wires. Elec. Power Syst. Res. 127, 206–212.

Brignone, M., Delfino, F., Procopio, R., Rossi, M., Rachidi, F., Tkachenko, S., 2012. An effective approach for high-frequency electromagnetic field-to-line coupling analysis based on regularization techniques. IEEE Trans. Electromagn. Compat. 54 (6), 1289–1297.

Brignone, M., Delfino, F., Procopio, R., Rossi, M., 2014. An equivalent two port model for a transmission line of finite length accounting for high frequency effects. IEEE Trans. Electromagn. Compat. 56 (6), 1657–1665.

Brignone, M., Delfino, F., Procopio, R., Rossi, M., Rachidi, F., 2017. Evaluation of power system lightning performance, part I: model and numerical solution using the PSCAD-EMTDC platform. IEEE Trans. Electromagn. Compat. 59 (1), 137–145.

Brignone, M., Delfino, F., Procopio, R., Rossi, M., Rachidi, F., 2017. Evaluation of power system lightning Performance—Part II: application to an overhead distribution network. IEEE Trans. on Electromagn. Compat. 59 (1), 146–153.

Chen, J., Zhu, M., 2014. Calculation of lightning flashover rates of overhead distribution lines considering direct and indirect strokes. IEEE Trans. Electromagn. Compat 56 (3), 668–674.

Datsios, Z.G., Mikropoulos, P.N., Tsovilis, T.E., 2014. Estimation of the minimum shielding failure flashover current for first and subsequent lightning strokes to overhead transmission lines. Elec. Power Syst. Res. 113, 141–150.

De Conti, A., Perez, E., Soto, E., Silveira, F.H., Visacro, S., Torres, H., 2010. Calculation of lightning-induced voltages on overhead distribution lines including insulation breakdown. IEEE Trans. Power Deliv. 25, 3078–3084.

Ekonomou, L., Gonos, I.F., Iracleous, D.P., Stathopulos, I.A., 2007. Application of artificial neural network methods for the lightning performance evaluation of Hellenic high voltage transmission lines. Elec. Power Syst. Res. 77 (January 1), 55–63.

Jinpeng, W., Bo, Z., Jinliang, H., Rong, Z., 2015. A comprehensive approach for transient performance of grounding system in the time-domain. IEEE Trans. Electromagn. Compat. 57, 250–256.

Maslowski, G., Wyderka, S., Ziemba, R., Karnas, G., Filik, K., Karpinski, L., 2016. Measurements and modeling of current impulses in the lightning protection system and internal electrical installation equipped with household appliances. Elec. Power Syst. Res. 139, 87–92.

Mikropoulos, P.N., Tsovilis, T.E., Koutoula, S.G., 2014. Lightning performance of distribution transformer feeding GSM base station. IEEE Trans. Power Deliv. 29, 2570–2579.

Minnaar, U.J., Gaunt, C.T., Nicolls, F., 2012. Characterisation of power system events on South African transmission power lines. Elec. Power Syst. Res. 88, 25–32.

Napolitano, F., Borghetti, A., Nucci, C.A., Martinez, M.L.B., Lopes, G.P., Dos Santos, G.J.G., 2014. Protection against lightning overvoltages in resonant grounded power distribution networks. Elec. Power Syst. Res. 113, 121–128.

Napolitano, F., Tossani, F., Nucci, C.A., Rachidi, F., 2015. The transmission-line approach for the evaluation of LEMP coupling to multi conductor lines. IEEE Trans. Power Deliv. 30 (2), 861–869.

Napolitano, F., Tossani, F., Borghetti, A., Nucci, C.A., Martinez, M.L., Lopes, G.P., Dos Santos, G.J., Fagundes, D.R., 2016. Lightning performance of a real distribution network with focus on transformer protection. Elec. Power Syst. Res. 139, 60–67.

International Standard IEC 62305-1 Protection against Lightning – Part 1: General Principles, first ed., 2006

International Standard IEC 62305-3 Protection against Lightning – Part 3: Physical Damage to Structures and Life Hazard, first ed., 2006

Statistical Digest 2014, Ceylon Electricity Board of Sri Lanka.

Visacro, S., Alipio, R., 2012. Frequency dependence of soil parameters: experimental results, predicting formula and influence on the lightning response of grounding electrodes. IEEE Trans. Power Deliv. 27, 927–935.

Visacro, S., Alipio, R., Vale, M.H.M., Pereira, C., 2011. The response of grounding electrodes to lightning currents: the effect of frequency-dependent soil resistivity and permittivity. IEEE Trans. Electromagn. Compat. 52, 401–406.

Visacro, S., Silveira, F.H., De Conti, A., 2012. The use of under built wires to improve the lightning performance of transmission lines. IEEE Trans. Power Deliv. 27.

Wu, J., He, J., Zhang, B., Zeng, R., 2016. Influence of grounding impedance model on lightning protection analysis of transmission system. Elec. Power Syst. Res. 139, 133–138.